

# On the Stability of Extrasolar Planetary Systems and other Closely Orbiting Pairs

Fred C. Adams<sup>1,2</sup> and Anthony M. Bloch<sup>3</sup>

<sup>1</sup>*Physics Department, University of Michigan, Ann Arbor, MI 48109*

<sup>2</sup>*Astronomy Department, University of Michigan, Ann Arbor, MI 48109*

<sup>3</sup>*Mathematics Department, University of Michigan, Ann Arbor, MI 48109*

October 2014

## ABSTRACT

This paper considers the stability of tidal equilibria for planetary systems in which stellar rotation provides a significant contribution to the angular momentum budget. We begin by applying classic stability considerations for two bodies to planetary systems — where one mass is much smaller than the other. The application of these stability criteria to a subset of the *Kepler* sample indicates that the majority of the systems are not in a stable equilibrium state. Motivated by this finding, we generalize the stability calculation to include the quadrupole moment for the host star. In general, a stable equilibrium requires that the total system angular momentum exceeds a minimum value (denoted here as  $L_X$ ) and that the orbital angular momentum of the planet exceeds a minimum fraction of the total. Most, but not all, of the observed planetary systems in the sample have enough total angular momentum to allow an equilibrium state. Even with the generalizations of this paper, however, most systems have too little orbital angular momentum (relative to the total) and are not in an equilibrium configuration. Finally, we consider the time evolution of these planetary systems; the results constrain the tidal quality factor of the stars and suggest that  $10^6 \lesssim Q_* \lesssim 10^7$ .

**Key words:** binaries: close — planets and satellites: dynamical evolution and stability — planetary systems — stars: kinematics and dynamics

## 1 INTRODUCTION

For two-body systems that include both rotational and orbital motion, the conditions required for the existence of a stable tidal equilibrium state have been determined (Darwin 1879, 1880; Counselman 1973; Hut 1980). This previous work shows that if the system can dissipate energy, for example through the action of tides, it can evolve in three possible ways: [1] The orbit of the secondary can move outward toward an unbound state, albeit at an ever-decreasing rate. [2] The orbit can decay inward and eventually collide with the primary. [3] The orbit can approach an equilibrium configuration characterized by equal periods for the orbit and spins of both bodies, circularization of the orbits, as well as alignment of the three angular momentum vectors.

In recent years, this classic problem has been the subject of renewed interest because it plays a role in a number of astrophysical contexts: Hot Jupiters can be destroyed via tidal dissipation by subgiants (Schlaufman & Winn 2013), and can spin up their parental stars as they spi-

ral inward (Zhang & Penev 2014). The tidal destruction of extrasolar planets – or lack thereof – can be used to place constraints on the tidal quality factor of the host stars (Penev et al. 2012). Similarly, a mass limit can be derived for hypothetical moons orbiting Jovian exoplanets (Barnes & O’Brien 2002). Many extrasolar planetary systems with Hot Jupiters (apparently) do not have an equilibrium state, and this complication changes the required description of their subsequent tidal evolution (Levrard et al. 2009). The alignment and evolution of planetary obliquity can also affect the habitability of planets (Heller et al. 2011). In addition to exoplanets, this issue arises in many other astronomical systems, including non-spherical binary asteroids (Scheeres 2002; Bellerose & Scheeres 2008; Scheeres 2009), common envelope evolution of binary stars (Taam & Sandquist 2000), the evolution of compact binary systems (Postnov & Yungelson 2006), and period gaps in binary millisecond pulsars (Taam et al. 2000).

This paper has two coupled goals. The first goal is to apply existing stability criteria to the planetary candi-

arXiv:1411.2859v1 [astro-ph.EP] 11 Nov 2014

dates discovered by the *Kepler* mission. The second goal is to generalize the stability criteria. Toward these ends, we first review the basic approach used in previous work (Counselman 1973; Hut 1980), and introduce notation appropriate for the extrasolar planetary systems of interest (Section 2). We apply these stability criteria to a subset of the *Kepler* sample for which stellar rotational periods are measured, and find that the majority of systems are not in a tidal equilibrium state (Section 3). Motivated by this finding, as well as the applications outlined above, Section 4 generalizes the classic problem of the stability of two-body systems containing spin angular momentum by augmenting the stellar potential to include a quadrupole term. However, this correction is small and the majority of the observed systems are not in a tidal equilibrium state. We deduce that the systems must still be evolving dynamically and consider the corresponding implications in Section 5; these results imply constraints on the tidal quality factor  $Q_*$  of the star. The paper concludes, in Section 6, with a summary and discussion of our results.

## 2 STABILITY OF PLANETARY SYSTEMS INCLUDING STELLAR SPIN

This section considers the equilibrium state of a two-body system consisting of a star and a single planet. To find this state, we need to extremize the system energy  $E$  subject to the constraint that the total angular momentum is constant. This treatment is parallel to that of previous work on binary stars (Hut 1980; Counselman 1973), and analogous to more general treatments of energy methods in stability problems (Wang et al. 1991; Simo et al. 1991).

In this system, both the energy and angular momentum budgets have contributions from three sources: the orbit, the spin of the star, and the spin of the planet. For the systems of interest here, the planets are small and have relatively little spin angular momentum; we thus reduce the problem by working in the limit where the planetary angular momentum vanishes. The orbit of the star-planet system can be described by the standard six orbital elements. In this case, however, we are only interested in the three variables  $(a, e, i)$  because the remaining ones can be averaged over; in other words, they only play a role on short timescales.

The star has moment of inertia  $I$  and spin angular momentum vector

$$\mathbf{S} = S\hat{z} \equiv I\Omega\hat{z}, \quad (1)$$

where the  $\hat{z}$  direction is coincident with the pole of the star and  $\Omega$  is the angular speed of the star. Following the treatment of Hut (1980), the total angular momentum of the system is conserved and is given by

$$\mathbf{L}(a, e, i, \Omega) = \mathbf{h} + I\Omega\hat{z}, \quad (2)$$

where  $\mathbf{h}$  is the orbital angular momentum, with magnitude  $h$  given by

$$h^2 = \mu^2 G(M+m)a(1-e^2), \quad (3)$$

where  $M$  is the stellar mass,  $m$  is the planetary mass, and  $\mu$  is the reduced mass<sup>1</sup> defined by

$$\mu = \frac{mM}{M+m}. \quad (4)$$

The direction of the orbital angular momentum vector is defined so that

$$\mathbf{h} \cdot \hat{z} = h \cos i. \quad (5)$$

The energy of the system is the sum of the orbital and spin energies, and is given by

$$E = -\frac{GMm}{2a} + \frac{1}{2}I\Omega^2. \quad (6)$$

Without loss of generality, we can define the direction of the orbital angular momentum vector so that

$$\mathbf{h} = (h \sin i, 0, h \cos i), \quad (7)$$

which thus defines the  $\hat{x}$ -axis. The total angular momentum vector  $\mathbf{L}$  can then be written

$$\mathbf{L} = (h \sin i, 0, h \cos i + I\Omega). \quad (8)$$

### 2.1 Extremum of the Energy

The basic problem is to find the extremum of the energy  $E$  given by equation (6) subject to the constraint that the total angular momentum  $\mathbf{L}$  (given by equation [8]) is constant. The energy is a function of four variables, including the semimajor axis  $a$ , the eccentricity  $e$ , the inclination angle  $i$ , and the spin rate  $\Omega$  of the star. The mass  $M$  of the star, mass  $m$  of the planet, and moment of inertia  $I$  are considered fixed. Since the angular momentum has only two nonzero components, we need two Lagrange multipliers (equivalently, the Lagrange multiplier is a two-dimensional vector). We thus introduce the two unknown quantities  $(\lambda_x, \lambda_z)$ . For each variable  $x_k$ , we get an optimization condition of the form

$$\frac{\partial E}{\partial x_k} + \lambda_x \frac{\partial}{\partial x_k}(h \sin i) + \lambda_z \frac{\partial}{\partial x_k}(h \cos i + I\Omega) = 0, \quad (9)$$

where the  $x_k$  are the four variables  $(a, e, i, \Omega)$ .

The above approach yields four equations that specify the tidal equilibrium state:

[1] For the semimajor axis  $a$ , the condition becomes

$$\frac{GMm}{a} + [\lambda_x \sin i + \lambda_z \cos i] h = 0. \quad (10)$$

[2] For the eccentricity  $e$ , optimization takes the form

$$[\lambda_x \sin i + \lambda_z \cos i] \frac{e}{1-e^2} = 0. \quad (11)$$

[3] For the inclination angle  $i$ , we obtain

$$\lambda_x h \cos i - \lambda_z h \sin i = 0. \quad (12)$$

[4] And finally for the rotation rate  $\Omega$  of the star, the constraint can be written

$$I\Omega + \lambda_z I = 0. \quad (13)$$

<sup>1</sup> Note that many different notations exist for the reduced mass: Here we follow Goldstein (1950) and use  $\mu$ ; compare with Murray & Dermott (1999) who use  $\mu^*$  and Morbidelli (2002) who uses  $\mu_1$ .

The eccentricity equation (11) implies that  $e = 0$ , and the other equations have solution  $i = 0$ ,  $\lambda_x = 0$ , and  $\lambda_z = -\Omega$ . The remaining condition thus becomes

$$\frac{GMm}{a} = \Omega h = \Omega \frac{Mm}{M+m} [G(M+m)a]^{1/2}. \quad (14)$$

As a result, the spin rate of the star must match the orbital angular velocity of the planet,

$$\Omega = \left[ \frac{G(M+m)}{a^3} \right]^{1/2}. \quad (15)$$

The total angular momentum is then given by

$$L = h + I\Omega = \frac{MmG^{2/3}}{(M+m)^{1/3}} \Omega^{-1/3} + I\Omega. \quad (16)$$

Given this expression, we see that  $L \rightarrow \infty$  in both limits  $\Omega \rightarrow 0$  and  $\Omega \rightarrow \infty$ . As a result, there exists a critical value of the total angular momentum  $L_X$ , such that no equilibrium exists for smaller values. This critical angular momentum is determined by finding the minimum of equation (16) as a function of  $\Omega$  and is given by

$$L_X = \frac{4}{3} \left[ \frac{3I(Mm)^3 G^2}{M+m} \right]^{1/4}. \quad (17)$$

At the critical point, the orbital angular momentum makes up three fourths of the total, whereas the stellar spin represents the remaining one fourth. This result is in agreement with that obtained earlier (Hut 1980).

## 2.2 Second Variation

In order for the system to be in equilibrium, the extremum found in the previous subsection must be a minimum of energy (rather than a maximum). Strictly speaking, the maximum only destabilizes in the presence of dissipation (Bloch et al. 1994); in the present application we expect dissipation over the long term, although it can be rather weak (see Section 5). If we use conservation of angular momentum,

$$\mathbf{L} = \mathbf{h} + I\Omega \hat{z}, \quad (18)$$

we can write the energy in the form

$$E = -\frac{GMm}{2a} + \frac{1}{2I} [L^2 + h^2 - 2Lh \cos \theta], \quad (19)$$

where  $\theta$  is the angle between the total angular momentum  $\mathbf{L}$  and the orbital angular momentum  $\mathbf{h}$ . Note that  $\theta$  is not the same as the inclination angle defined earlier, but we can use  $\theta$  as the third variable and find that  $\theta = i = 0$  in the equilibrium state (Hut 1980).

After some algebra, the second derivatives, evaluated at the equilibrium conditions, have the forms

$$\frac{\partial^2 E}{\partial a^2} = \frac{GMm}{4a^3} \left[ -3 + \frac{\mu a^2}{I} \right], \quad (20)$$

$$\frac{\partial^2 E}{\partial e^2} = \frac{GMm}{a}, \quad (21)$$

and

$$\frac{\partial^2 E}{\partial \theta^2} = \frac{GMm}{a} \left[ 1 + \frac{\mu a^2}{I} \right]. \quad (22)$$

Since all of the off-diagonal terms vanish at the equilibrium state, these three second-partial-derivatives also define the eigenvalues of the relevant Hessian matrix (Hesse 1872). The second two expressions are manifestly positive. The only nontrivial constraint required for stability is that the first expression (from equation [20]) is positive, which implies

$$\frac{\mu a^2}{I} > 3. \quad (23)$$

At the critical point, the orbital angular momentum has the form  $h = \mu a^2 \Omega$ , so the above constraint can be written in the alternate form

$$h = \mu a^2 \Omega > 3I\Omega. \quad (24)$$

In other words, the orbital angular momentum must be three times larger than the spin angular momentum in order for the system to be in its stable equilibrium state (in agreement with the results of Hut 1980 in the limit where the companion has no spin). Notice also that since  $L = h + I\Omega$ , the above condition can be written in the alternate form  $h > 3L/4$ .

## 2.3 Stability and Instability

The meaning of the tidal equilibrium state derived above can be illustrated by considering the system energy as a function of angular momentum, or, equivalently, semi-major axis. First we define the dimensionless energy and orbital angular momentum according to

$$\mathcal{E} \equiv \frac{E}{(L_X^2/2I)} \quad \text{and} \quad \eta \equiv \frac{h}{L_X}. \quad (25)$$

Next we specialize to the case where the spin of the star is aligned with the direction of the orbit and the eccentricity vanishes (note that  $i = 0 = e$  is necessary for equilibrium). The energy from equation (19) then has the form

$$\mathcal{E} = -\frac{27}{256} \frac{1}{\eta^2} + (\ell - \eta)^2, \quad (26)$$

where we have defined  $\ell \equiv L/L_X$ . We then plot the energy as a function of (dimensionless) orbital angular momentum, as shown in Figure 1. For  $\ell \leq 1$ , no equilibria are possible, and the energy is a monotonic function of  $\eta$ . For  $\ell > 1$ , the energy curve has a stable equilibrium point at some value  $\eta_+ > 1$  and an unstable equilibrium point at  $\eta_- < 1$ . Planetary systems with a given value of total angular momentum ( $\ell$ ) will fall on the corresponding energy curve in this diagram. If their location falls to the left of the local maximum, the planet can spiral inward and would eventually be accreted.

Next we want to delineate the parts of parameter space that lead to stable and unstable configurations. The binary systems considered here have a large number of parameters, including the masses  $m$  and  $M$ , the stellar rotation rate  $\Omega$ , the moment of inertia  $I$ , and the orbital elements  $(a, e, i)$  of the secondary. Since we are primarily interested in planetary systems, we can fix the stellar properties, which are chosen (for now) to be those of the Sun. For the sake of definiteness, we also consider circular orbits in the plane ( $e = 0 = i$ ). Some systems will have smaller stars and different rotation rates, but

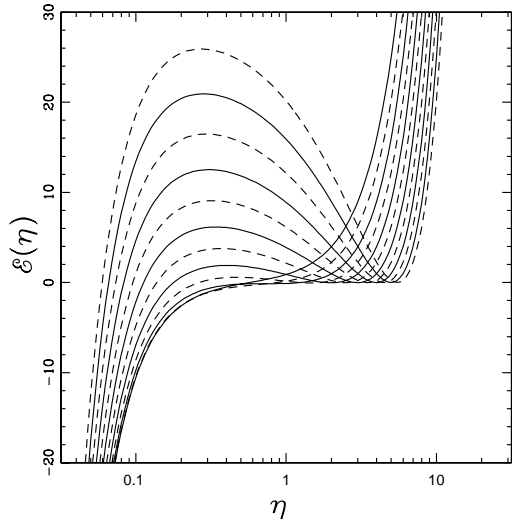


**Figure 1.** Total system energy as a function of dimensionless orbital angular momentum. Energy curves are shown for a range of total angular momenta  $\ell = L/L_X$ , which are equally spaced. From bottom to top, the solid curves correspond to  $\ell = 1, 2, 3, 4,$  and  $5$ ; the dashed curves show  $\ell = 3/2, 5/2, 7/2, 9/2,$  and  $11/2$ . Planetary systems (with no external torques) conserve angular momentum and must follow these paths. In systems that start to the left of the local maximum, the planet spirals inwards; in systems that start to the right of the maximum, the planet spirals outward until it reaches the local minimum of energy.

these differences have less dynamic range than those of the planet masses and semimajor axes. The parameter space thus reduces to  $(a, m)$ .

With the above specifications, we plot the regions of stability in the  $m$ - $a$  plane in Figure 2. The semimajor axes  $a$  are given in units of the stellar radius and the planet masses are expressed relative to the mass of Jupiter. This diagram shows that planetary systems can be unstable for different reasons. The area to the left of the solid red curve delineates the parameter space for which the systems have too little total angular momentum ( $L < L_X$ ) so that no equilibrium state is possible; this condition is denoted here as type-I instability. The area below the dashed blue line delineates the parameters for which the systems have too little orbital angular momentum relative to the spin (so that  $h < 3S$ ); this condition is denoted as type-II instability. Note that systems can fail both requirements and be unstable for two reasons (for parameters in the middle left part of the plot). The upper right portion of the diagram delineates the parameters for which the systems are stable. Note that systems with Jovian planets are susceptible to type-I instability (not enough total angular momentum), whereas smaller planets are more likely to suffer type-II instability (not enough orbital angular momentum). In this context, small planets are those with lower masses than Neptune.

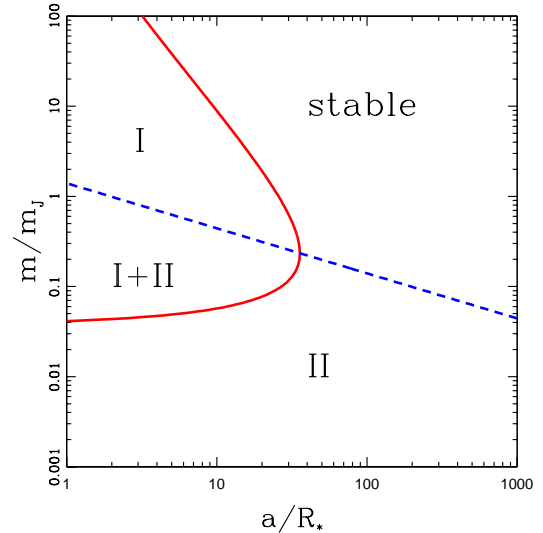


**Figure 2.** Regions of stability and instability for systems where the primary has solar properties. The horizontal axis marks the semimajor axis of the orbit (in units of solar radii) and the vertical axis marks the mass of the secondary (in Jupiter masses). In the region to the left of the solid red curve (region I), the systems fail to have enough total angular momentum for tidal equilibrium ( $L < L_X$ ); in the region below the blue dashed line (region II), systems fail to have enough orbital angular momentum ( $h < 3S$ ). Stable orbits fall in the upper right portion of the plane.

Note that for smaller stars (and/or slower rotation rates), the region of type-I instability will be larger.

### 3 APPLICATION TO KEPLER PLANETS

This section uses the stability criteria outlined above to analyze a subset of the *Kepler* sample of extrasolar planet candidates (Batalha et al. 2013). In order to apply the stability conditions, the rotation rates of the host stars must be known. Toward that end, we use the results of McQuillan et al. (2013), who detected rotational periods for 797 of the stars that host *Kepler* objects of interest. This set of systems is reduced further by eliminating known eclipsing binaries, previously published blended objects, systems that are likely to be eclipsing binaries, and systems whose centroid motions indicate rotation and transit modulation on different stars (for further detail, see McQuillan et al. 2013). With this reduction, the sample contains 738 planetary systems. Within the sample, we consider only the innermost planetary candidates, which are then assumed to be real with their reported radii and orbital elements. For the sake of definiteness, we convert planetary radii to masses using the relation  $m = M_{\oplus} (R_p/R_{\oplus})^{2.1}$  (Lissauer et al. 2011), which is appropriate for smaller planets ( $m < 150M_{\oplus}$ ; for example, see Weiss et al. 2013 and references therein). The orbital eccentricities are not generally measured and are

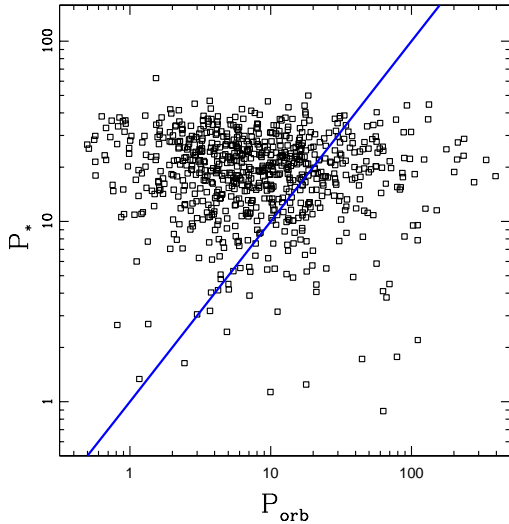


**Figure 3.** Stellar rotation period versus orbital period of the innermost planet for *Kepler* candidates (see Batalha et al. 2013; McQuillan et al. 2013). The blue line depicts equal periods. Note that the systems do not generally exhibit synchronicity.

set to zero for this analysis. For the stars, in addition to their reported properties, we assume that the dimensionless moment of inertia has a single value  $\chi = I/(MR^2) = 0.10$ , which is intermediate between that of a fully convective  $n = 3/2$  polytrope and a fully radiative  $n = 3$  polytrope (e.g., see Figure 2 of Batygin & Adams 2013). Note that the correction for nonzero eccentricity is  $\mathcal{O}(e^2)$  and that the moment of inertia dependence has the form  $L_X \propto I^{1/4}$  (see equation [17]), so that the results presented below are relatively insensitive to these approximations.

First we plot the stellar rotation period versus the orbital period of the innermost planet, as shown in Figure 3 (which is analogous to Figure 2 of McQuillan et al. 2013). This figure shows immediately that the observed planetary systems are not synchronous in general, and hence are not in stable equilibrium states. The diagonal blue line in the figure shows the locus of equal periods. Note that the data fall on both sides of this line of synchronicity. Although more points fall above the line, the transits are more likely to be observed for shorter orbital periods, so selection effects could account for this asymmetry. Another interesting feature of Figure 3 is that it shows no apparent correlation between the stellar rotation period and the orbital period. In other words, the data points do not cluster around the expected line of synchronicity, but rather appear to be completely independent.

Given that the planetary systems are not in a co-rotating state, which is required for equilibrium, the next step is to determine if such an equilibrium exists. The result is shown in Figure 4. The vertical axis plots the ratio of the total (spin plus orbit) angular momentum of the

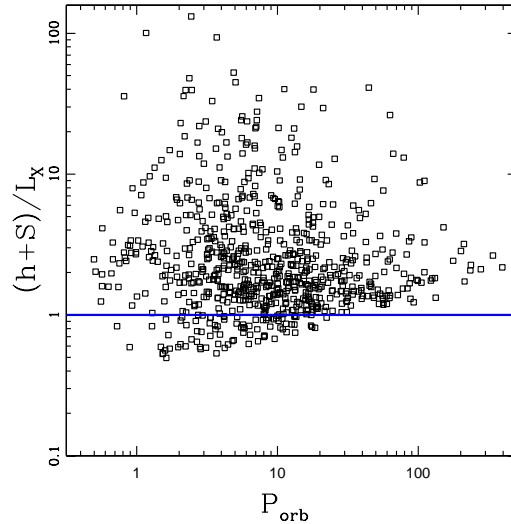


**Figure 4.** Ratio of the total angular momentum to the critical value, plotted as a function of orbital period. Only systems with sufficient angular momentum, those above the blue line in the figure, have a tidal equilibrium state. The area below the line corresponds to region I instability from Figure 2. The 85 systems (out of 738) that fall below the horizontal blue line have no tidal equilibrium state.

system to the minimum value  $L_X$  needed for the existence of an equilibrium state (see equation [17]). This ratio is plotted versus orbital period of the planet. Even though most systems are not in tidal equilibrium (as indicated by Figure 3), an equilibrium state does exist for the majority of the cases (most systems lie above the critical line). Nonetheless, 85 systems (out of 738 total) fall below the critical blue line in Figure 4. These systems have no accessible equilibrium state and are subject to type-I instability (see Figure 2); these planets must eventually either spiral inward or outward.

Although a sizable majority (653 out of 738) of the planetary systems in the sample have enough angular momentum for a tidal equilibrium state (Figure 4), only a small fraction of the systems are in a synchronous state within the observational uncertainties (synchronicity is one of the conditions to be in stable equilibrium). Another requirement to be in stable equilibrium is for the orbital angular momentum  $h$  to represent a sufficiently large fraction of the total  $L$ . For the case of no quadrupole ( $q \rightarrow 0$ ), this condition can be written as  $h > 3L/4$ , or, equivalently,  $h > 3S$ . As expected, the ratio  $h/S$  is generally smaller than indicated by this requirement, as shown in Figure 5. In fact, most of the systems have far too little orbital angular momentum, relative to spin angular momentum, to be in stable equilibrium.

Note that most members of both the *Kepler* sample considered here and the set of Hot Jupiters considered previously (Levrard et al. 2009) fail to reside in their tidal equilibrium states. However, the two sets of planetary systems are dynamically different: The Hot Jupiter

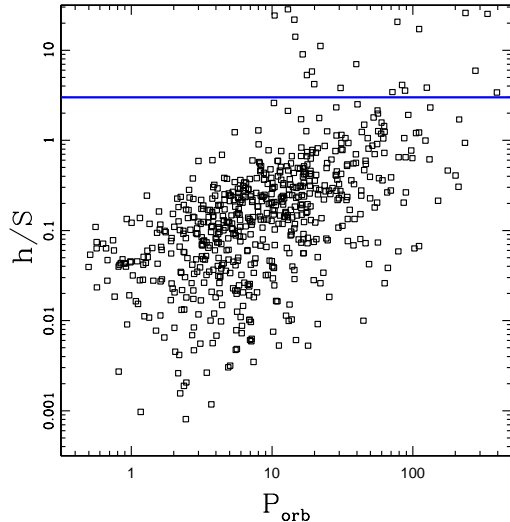


**Figure 5.** Ratio of the orbital angular momentum  $h$  to the spin angular momentum  $S$  of the star, plotted here as a function of orbital period. Only systems with  $h/S > 3$ , those above the blue line in the figure, can reside in their tidal equilibrium state. The area below the line corresponds to region II instability in Figure 2. This plot shows that the majority of planetary systems in the sample are not in equilibrium. Only the systems for which the equilibrium state exists (those with  $L > L_X$ ) are included in the plot.

systems generally have too little total angular momentum, so that the constraint  $L > L_X$  is not satisfied; they are thus subject to type-I instability (see Figure 2). In contrast, the *Kepler* systems considered here generally have enough total angular momentum (Figure 4), but not enough orbital angular momentum (Figure 5), and are subject to type-II instability. This difference arises due to the difference in planetary masses in the two samples. The *Kepler* systems generally have much smaller masses, so that the critical angular momentum  $L_X \propto m^{3/4}$  is smaller and the constraint  $L > L_X$  is more easily satisfied. On the other hand, the orbital angular momentum  $h \propto m$  is smaller for these low mass planets, and the constraint  $h > 3L/4$  is more difficult to meet.

The considerations of the Section 2 show that stability requires two conditions, which can be written in the form

$$\frac{h}{L} > \frac{3}{4} \quad \text{and} \quad L > L_X = \frac{4}{3} \left[ \frac{3IG^2(Mm)^3}{M+m} \right]^{1/4}. \quad (27)$$

To apply these criteria to observed systems, however, we must know both the orbital angular momentum and the spin angular momentum. The latter quantity requires additional measurements of stellar properties (to find the rotation rate) and these are not always available. It is useful to derive a combined constraint that does not require data for stellar rotation rates. We can combine the two constraints in equation (27) to obtain the weaker condition

$$h > \frac{3}{4} L_X = \left[ \frac{3IG^2(Mm)^3}{M+m} \right]^{1/4}. \quad (28)$$

This constraint can be written in the alternate form

$$a > \left[ \frac{3I}{\mu} \right]^{1/2}. \quad (29)$$

We can write the moment of inertia of the star in the form  $I = \chi MR^2$ , which defines the parameter  $\chi$  (and where we expect  $\chi \approx 0.10$  for Solar-type stars). With this definition, the constraint for stability becomes

$$a > \left[ 3\chi \frac{M}{\mu} \right]^{1/2} \quad R \equiv R_C, \quad (30)$$

where the second equality defines the weighted stellar radius  $R_C$ . For example, for Jovian planets,  $\mu/M \approx 10^{-3}$ , so the constraint takes the form  $a > R_C \approx 13R_*$ .

The constraint of equation (30) is necessary but not sufficient. Any planetary system in equilibrium must satisfy the constraint, but it remains possible for systems to satisfy the inequality and still not be in tidal equilibrium. These latter systems would not satisfy the requirement that  $h/S > 3$ . This issue is illustrated in Figure 6, which shows the ratio  $a/R_C$  plotted versus the ratio  $h/S$  for all of the systems in the sample that have enough angular momentum to allow for an equilibrium state (i.e., for the systems with  $L > L_X$ ). The blue lines in the figure delineate the regions where  $h > 3S$  and  $a > R_C$ . The simplified constraint of equation (30) does a reasonable job of specifying the systems that are not in equilibrium. Nonetheless, 24 systems (out of 653) lie above the horizontal blue but do not fall to the right of the vertical line, i.e., they do not satisfy  $h > 3S$ .

Figures 3 – 6 suggest that the majority of *Kepler* systems (those in the sample defined above) have enough angular momentum to allow the existence of a tidal equilibrium state, but are not actually in a stable equilibrium. Compared to the conditions required for stability, the orbital periods are not commensurate with the stellar spin periods and the orbital angular momenta are too small relative to the stellar spin angular momenta. For most systems, the star spins more slowly than the planet orbits around it (see Figure 3), so that the action of tidal evolution will move the orbits inward toward the star. Since the systems already have too little orbital angular momentum, these planets are scheduled for accretion and hence destruction. For roughly 1/3 of the systems, however, the star spins faster than the orbit, and tidal torques will act to move the planets outward.

The above point can be illustrated by plotting the observed planetary systems on the energy curves defined by equation (26). For each system, we find the total angular momentum  $L$ , the critical angular momentum  $L_X$ , the ratio  $\ell = L/L_X$ , and the dimensionless orbital angular momentum  $\eta = h/L_X$ . The reduced energy from equation (26) is plotted as a function of  $\eta$  in Figure 7. The collection of energy curves shown in the figure correspond to discrete values of the total system angular momentum  $\ell = L/L_X = 1, 2, 3, 4$ , and 5, where the largest  $\ell$  value produces the largest local maximum. The heavy red solid curve shows the locations of these maxima for continuous  $\ell \geq 1$ . For systems in which the star

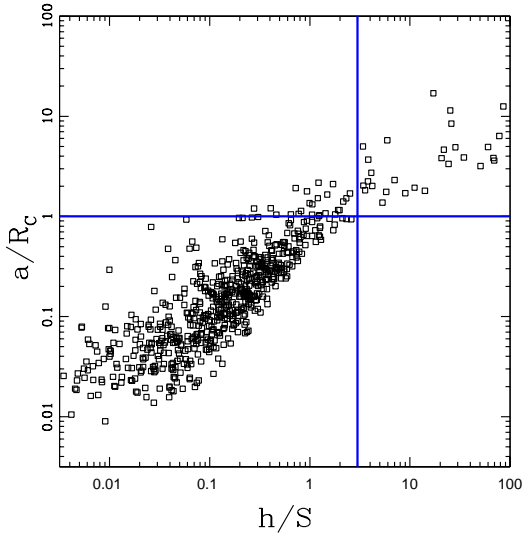


**Figure 6.** Comparison of two stability criteria. The simplified condition  $a/R_C > 1$  is necessary but not sufficient, whereas the stricter criterion  $h/S > 3$  requires that the stellar rotation rates are measured. Most — but not all — of the systems that satisfy the weaker constraint (and lie above the horizontal line) also satisfy the stronger constraint (and lie to the right of the vertical line).

spins faster than the orbital angular velocity, the points (depicted by open squares) fall to the right of this locus of maxima. Similarly, for systems where the star spins more slowly than the orbit, the points (solid triangles) fall to the left. As a result, systems that fall to the right of this locus will spiral outward due to tidal interactions with the star and thereby move toward the tidal equilibrium state. Systems that fall to the left of the locus must spiral inward to move toward lower system energies, but no equilibrium state can be reached. Within the context of this model, the planets continually spiral inward. In practice, however, these curves should be truncated on the left hand side: For a given system, there exists a minimum orbital angular momentum necessary to keep the planet in orbit outside the star.

Figure 7 shows that more planets will spiral outward (and hence survive) than the number of planets that already meet the constraint  $h > 3I\Omega$  (compare with Figure 5). This ordering makes sense: The requirement that the system has enough orbital angular momentum to evolve toward an equilibrium state is less stringent than the requirement  $h > 3I\Omega$  necessary for the system to reside in a tidal equilibrium state.

We note that the interpretation used throughout this section implicitly assumes that the stars are spinning in nearly solid-body rotation with a well defined rate that is measured at the surface. It remains possible for only the outer layers of the star to participate in rotation, so that the effective stellar moment of inertia is smaller than expected, perhaps by a factor of  $\sim 10$  (see also Levrard et al. 2009). If this were the case, the spin angu-

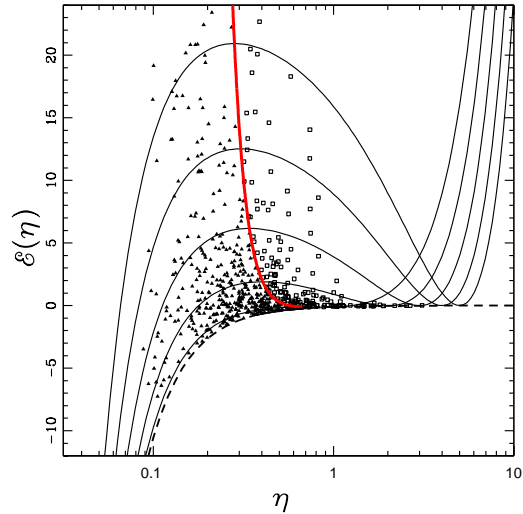


**Figure 7.** Energy versus orbital angular momentum for the sample of observed planetary systems. The energy curves are plotted for discrete values of total dimensionless angular momentum  $\ell = 1, 2, 3, 4,$  and  $5$  (from bottom to top). The filled triangles depict systems for which the star is rotating more slowly than the orbit, whereas the open squares depict cases where the star is rotating more quickly. The heavy solid red line shows the locus of maxima for the energy curves. The heavy dashed curve shows the energy function in the limit of zero stellar spin and delineates the lower boundary of the region accessible to planetary systems.

lar momentum would be smaller, and more of the systems could be in stable equilibrium states.

#### 4 PLANETARY SYSTEMS WITH STELLAR SPIN AND QUADRUPOLE MOMENT

The conditions for tidal equilibrium can be generalized to include the quadrupole moment of the star. This generalization is interesting for several reasons. The previous section shows that for one particular sample, most planetary systems do not reside in a tidal equilibrium state; we would thus like to know if the inclusion of the quadrupole moment moves the theoretical equilibrium toward the data (on average). In addition, the quadrupole term leads to the precession of orbits. This effect, in turn, affects transit timing variations for orbits with nonzero eccentricity and/or inclination (Agol et al. 2005; Holman & Murray 2005), as well as efforts to measure stellar quadrupole moments (Miralda-Escudé 2002). Finally, both the quadrupole and the general relativistic correction to the potential (Hartle 2003) have the same

radial dependence ( $\Phi \propto 1/r^3$ ), so this derivation informs the corresponding relativistic problem.<sup>2</sup>

This treatment considers the particular case where the planetary orbit is circular (so that  $e = 0$ ) and lies in the plane defined by the stellar spin axis (so that  $i = 0$ ). Note that these conditions ( $e = 0 = i$ ) are assumed here, but are required for the tidal equilibrium states derived in Section 2. Notice also that most planetary candidates with tight orbits tend to have small or vanishing eccentricity. For systems in this state, the orbital radius and semimajor axis coincide, so that  $r = a$  over the entire orbit. In this case, the gravitational potential (e.g., see Hartle 2003) reduces to the form

$$\Phi = -\frac{GM}{r} - \frac{GQ_\Phi}{r^3}. \quad (31)$$

Note that the parameter  $Q_\Phi$  can also be written in the form  $Q_\Phi = (1/2)J_2MR^2$ , so that  $Q_\Phi$  has the same units as the moment of inertia. With this specification, the energy  $E$  of the system can be written as

$$E = -\frac{GMm}{2a} + \frac{GQ_\Phi m}{2a^3} + \frac{1}{2}I\Omega^2. \quad (32)$$

Note that the quadrupole moment of the star will also produce a change in the stellar moment inertia  $I$  and can lead to precession of the spin axis; for the co-planar systems of interest here, however, we can ignore precession and simply use the modified value of  $I$ . The angular momentum of the system points in the  $\hat{z}$  direction and has magnitude  $L = h + I\Omega$ , where the orbital angular momentum  $h$  has the form

$$h^2 = \mu m \left[ GMa + \frac{3GQ_\Phi}{a} \right]. \quad (33)$$

For circular orbits, this expression follows from the specification of the potential in equation (31) and the definition of orbital angular momentum (see also Danby 1968).

#### 4.1 Extremum of the Energy

To find the extremum of the energy, subject to the angular momentum being constant, we find the derivatives of the composite function  $F = E + \lambda L$  where  $\lambda$  is the (single) Lagrange multiplier in the problem. We are left with only two variables, the semimajor axis  $a$  of the orbit and the stellar rotation rate  $\Omega$ .

[1] For the semimajor axis  $a$ , the derivative  $\partial F/\partial a$  provides the condition

$$\frac{GMm}{2a^2} - \frac{3GQ_\Phi m}{2a^4} + \lambda \frac{\mu m}{2h} \left[ GM - \frac{3GQ_\Phi}{a^2} \right] = 0. \quad (34)$$

[2] For the stellar spin rate  $\Omega$ , the derivative  $\partial F/\partial \Omega$  provides the condition

$$I\Omega + \lambda I = 0. \quad (35)$$

The second condition implies that  $\lambda = -\Omega$ . Using this specified value of the Lagrange multiplier, the remaining constraint of equation (34) can be written in the form

<sup>2</sup> However, we note that the relativistic version of this additional term depends on the angular momentum, so that the two problems are not equivalent.

$$\left[ \frac{1}{a^2} - \Omega \frac{\mu}{h} \right] \left[ M - \frac{3Q_\Phi}{a^2} \right] = 0. \quad (36)$$

Formally, each of the factors could vanish and thereby satisfy the constraint. However, the parameter  $Q_\Phi$  can be written in the form  $Q_\Phi = (1/2)J_2MR^2$ , where  $R$  is the stellar radius and the dimensionless parameter  $J_2 \ll 1$ . We also expect  $R \ll a$ . As a result, for almost all realistic systems  $M \gg 3Q_\Phi/a^2$ , so that the second factor is nonzero and can be divided out. This leaves us with the requirement

$$h = \mu\Omega a^2. \quad (37)$$

Using the definition of the orbital angular momentum  $h$ , one finds

$$\mu m \left[ GMa + \frac{3GQ_\Phi}{a} \right] = \mu^2 \Omega^2 a^4, \quad (38)$$

which reduces to the form

$$\Omega^2 = \frac{G(M+m)}{a^3} \left[ 1 + \frac{3Q_\Phi}{Ma^2} \right]. \quad (39)$$

In the limit  $Q_\Phi \rightarrow 0$ , we recover the previous result from equation (15). Even for  $Q_\Phi \neq 0$ , however, equation (39) represents synchronous rotation: The correction factor for the stellar spin rate is the same factor by which the orbital angular velocity changes with the introduction of a quadrupole moment (for circular orbits). Finally, we note that the correction to the rotation rate is  $\mathcal{O}(J_2R^2/a^2) \ll 1$ . In practice, the size of this correction term will often be much less than the uncertainties in the estimates of the stellar masses (which are notoriously difficult to determine).

#### 4.2 Minimum Total Angular Momentum

The total angular momentum  $L = h + I\Omega$ . Whereas in the previous case we could invert the analog of equation (39) and write  $a$  in terms of  $\Omega$ , in this case it is easier to eliminate  $\Omega$ . After some rearrangement the total angular momentum becomes

$$L = \left[ 1 + \frac{3Q_\Phi}{Ma^2} \right]^{1/2} (GMm\mu)^{1/2} \left\{ a^{1/2} + \frac{I}{\mu a^{3/2}} \right\}. \quad (40)$$

We can solve for the critical value of  $a$  for which the angular momentum is minimized, i.e.,

$$a_{\min}^2 = \frac{I}{2\mu} \left\{ 3 + 3q + [9 + 78q + 9q^2]^{1/2} \right\}, \quad (41)$$

where we have defined the dimensionless parameter

$$q \equiv \frac{\mu Q_\Phi}{MI}. \quad (42)$$

Note that  $q \ll 1$ . Using the critical value of the semimajor axis, we can then find the minimum value of the angular momentum, which can be written in the form

$$L_X = \left[ \frac{G^2(Mm)^3 I}{(M+m)} \right]^{1/4} f(q), \quad (43)$$

where we have defined the dimensionless function

$$f(q) \equiv \left\{ 5 + 3q + [9 + 78q + 9q^2]^{1/2} \right\} \quad (44)$$

$$\times \frac{\left\{3 + 9q + [9 + 78q + 9q^2]^{1/2}\right\}^{1/2}}{2^{1/4} \left\{3 + 3q + [9 + 78q + 9q^2]^{1/2}\right\}^{5/4}}.$$

Since  $q \ll 1$ , we can find the leading order correction. After expanding we thus obtain

$$f(q) = \frac{4}{3^{3/4}} \left\{1 + \frac{1}{2}q + \mathcal{O}(q^2)\right\}. \quad (45)$$

In the limit  $q \rightarrow 0$ , the function  $f(q)$  reduces to

$$f(q) \rightarrow \frac{4}{3^{3/4}}. \quad (46)$$

As a result, in this limit we recover the solution obtained previously for the case where the potential has no quadrupole term (as expected).

### 4.3 Second Variation

After eliminating the stellar spin variable, we can write the energy of the system in the form

$$E(a) = -\frac{GMm}{2a} + \frac{GQ_{\Phi}m}{2a^3} + \frac{1}{2I} (L^2 + h^2 - 2Lh), \quad (47)$$

where  $L$  is the total angular momentum and  $h$  is the orbital angular momentum given by equation (33). The first derivative can be written

$$\frac{dE}{da} = \frac{GMm}{2a^2} - \frac{3GQ_{\Phi}m}{2a^4} + \frac{1}{I} (h - L) \frac{dh}{da} = 0, \quad (48)$$

and the second derivative becomes

$$\begin{aligned} \frac{d^2E}{da^2} = & -\frac{GMm}{a^3} + \frac{6GQ_{\Phi}m}{a^5} \\ & + \frac{1}{I} \left[ \left( \frac{dh}{da} \right)^2 + (h - L) \frac{d^2h}{da^2} \right]. \end{aligned} \quad (49)$$

After some algebra, we can write the requirement that the second derivative is positive in the form

$$\begin{aligned} \left[ - \left( 1 + 3q \frac{L-h}{h} \right) + \frac{L}{4(L-h)} \left( 1 - 3q \frac{L-h}{h} \right) \right] \\ \times \left[ 1 - 3q \frac{L-h}{h} \right] > 0, \end{aligned} \quad (50)$$

where we have used the dimensionless parameter  $q$  defined by equation (42). The second factor is positive for small  $q$ , but in general requires the (rather weak) constraint

$$h > \frac{3q}{1+3q} L. \quad (51)$$

Positivity of the remaining factor requires that

$$hL(1+3q) - 3qL^2 > 4(L-h)[h(1-3q) + 3qL], \quad (52)$$

which can be solved to find the constraint

$$\frac{h}{L} > g(q), \quad (53)$$

where the function  $g(q)$  is defined as

$$g(q) \equiv \frac{3(1-9q) + [9(1-9q)^2 + 240q(1-3q)]^{1/2}}{8(1-3q)}. \quad (54)$$

To leading order, we can write

$$\frac{h}{L} > \frac{3}{4} \left\{ 1 + \frac{2}{3}q + \mathcal{O}(q^2) \right\}. \quad (55)$$

In the limit  $q \rightarrow 0$ , this constraint reduces to the now-familiar form  $h/L > 3/4$ . Note that the constraint of equation (53) is much more stringent than that of equation (51).

Equations (53 – 55) show that the inclusion of the quadrupole term results in a tighter constraint: A larger fraction of the total angular momentum must reside in the orbit. For the observational sample of Section 3, however, this correction is small. The parameter  $q = (\mu/M)(Q_{\Phi}/I) = (\mu/M)(J_2/2)$ . The first factor is typically  $\mu/M \sim 10^{-4}$  and the second factor  $J_2/2 \sim 10^{-6}$ , so the correction is not large enough to move the observed planetary systems out of (or into) equilibrium states.

For completeness we note that the results of this section can be useful in other settings. For example, the dwarf planet Haumea has a large effective  $J_2 \approx 0.24$  (Ragozzine & Brown 2009) due its rapid spin and asymmetrical shape, where this  $J_2$  value is obtained by time-averaging a rapidly rotating ellipsoid with the observed axis ratios. In addition, the dwarf planet has two large satellites, Namaka and Hiiaaka, which have experienced an interesting dynamical history (Ćuk et al. 2013). The results of this section can be used to describe the tidal equilibrium states of this system, and others.

### 4.4 Size of the Planetary Spin Term

The treatment thus far has neglected the spin of the planet. In the equilibrium state, the planet is expected to have a spin rate that is synchronous with its orbital angular velocity. It is useful to compare the size of the additional energy term due to the quadrupole moment with that due to the planetary spin. We can write the ratio in the form

$$\mathcal{R}_{\text{qs}} = \frac{GQ_{\Phi}m}{2a^3} \frac{2}{I_P \Omega^2} = \frac{Q_{\Phi}m}{I_P M}. \quad (56)$$

If the planet and the star have the same internal structure, then  $I_P = (mR_P^2/MR^2)I$ , where  $I$  is the stellar moment of inertia. The ratio of energy terms then becomes

$$\mathcal{R}_{\text{qs}} = \frac{Q_{\Phi}}{I} \left( \frac{R}{R_P} \right)^2 \approx 100 \frac{Q_{\Phi}}{I}. \quad (57)$$

It is thus possible for the spin term to dominate the quadrupole term, or for the two terms to have comparable sizes ( $\mathcal{R}_{\text{qs}} \sim 1$ ).

Fortunately, we can readily incorporate planetary spin into our previous results: Since the extremum condition requires that both bodies and the orbit have the same angular velocity, the rotation energy and angular momentum are generalized to the forms

$$K_R = \frac{1}{2} I \Omega^2 + \frac{1}{2} I_P \Omega^2 \quad \text{and} \quad L_S = I \Omega + I_P \Omega, \quad (58)$$

where  $I$  is the stellar momentum of inertia and  $I_P$  is the planetary moment of inertia. As a result, we can incorporate the effects of planetary spin by making the substitution

$$I \rightarrow I + I_P. \quad (59)$$

This generalized expression should be used for the moment of inertia in equations (17) and (43).

## 5 TIME EVOLUTION

Even with the generalization of the stability criteria considered in Sections 4, the majority of the systems in the sample are not in a tidal equilibrium state. One explanation for this finding is that the systems are still evolving, but the relevant time scales are long. More specifically, we expect tidal interactions between the planets and their host stars to cause them to spiral inward (outward) when the stellar spin is slower (faster) than the angular velocity of the orbit. For most systems, the orbital angular speed is larger than the stellar spin (Figure 3) so that planets are expected to be accreted in the long run. Because the planets are still observable, however, the time scale for them to spiral into their stars must be longer than the typical age of the systems.

To test this hypothesis, we consider the time required for a planet to spiral inward due to tidal dissipation in the star. Because the coefficient that sets the magnitude of this effect, the value of  $Q_*$ , is highly uncertain, we consider a simple model where the semimajor axis of the planet evolves according to

$$\frac{d}{dt} \left( \frac{a}{a_0} \right) = -\tau_*^{-1} \left( \frac{\Omega_{\text{orb}} - \Omega}{\Omega_{\text{orb}}} \right) \left( \frac{a}{a_0} \right)^{-11/2}. \quad (60)$$

This form follows from previous work (e.g., Goldreich & Soter 1966; Hut 1981). In particular, we start from equation (3) of Levrard et al. (2009) and take the limiting form where the eccentricity is zero and the system is aligned. The factor  $(\Omega_{\text{orb}} - \Omega)/\Omega_{\text{orb}}$  takes into account the difference between the spin rate of the star and the angular speed of the orbit (this factor approaches unity when the star spins slowly compared to the orbit). The time scale  $\tau_*$  is given by

$$\tau_* \equiv \frac{2}{9} Q_* \frac{M}{m} \left( \frac{a_0}{R} \right)^5 \left( \frac{a_0^3}{GM} \right)^{1/2}, \quad (61)$$

where  $a_0$  is the starting value of the semimajor axis and  $R$  is the stellar radius. Note that the definition of the tidal dissipation parameter  $Q_*$  varies by dimensionless factors of order unity in different treatments (e.g., compare Goldreich & Soter 1966; Hut 1981; Adams & Laughlin 2006; Levrard et al. 2009). Given the above definitions, the equation of motion is readily integrated to obtain the solution

$$a(t) = a_0 \left[ 1 - \frac{13}{2} \frac{t}{\tau_*} \right]^{2/13}, \quad (62)$$

where we have taken the limit  $(\Omega_{\text{orb}} - \Omega)/\Omega_{\text{orb}} \rightarrow 1$ . The total (possible) evolution time is thus given by  $t_{\text{evol}} = (2/13)\tau_*$  (see also Adams & Laughlin 2006). In practice, however, the planet will strike the stellar surface at an earlier time  $t = (2/13)\tau_* [1 - (R/a_0)^{13/2}]$ . The correction is small: For a typical close planet with a 4-day orbit, the difference between  $t_{\text{evol}}$  and the true evolution time is less than one part in a million. As a result, we can

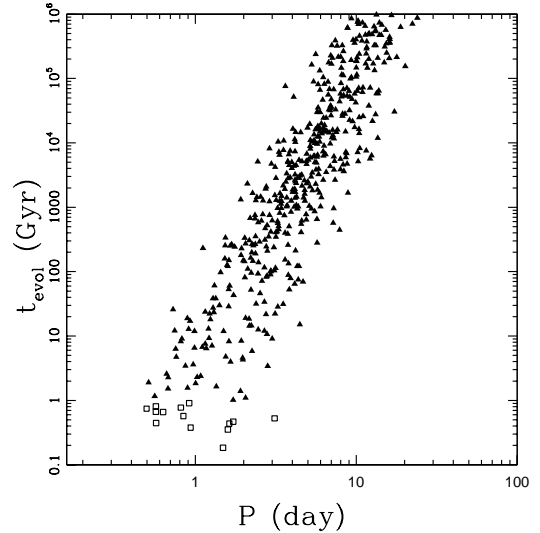


**Figure 8.** Estimated time for planets to spiral into their host star (plotted here versus current orbital period). Timescales are calculated assuming  $Q_* = 10^6$ .

ignore this complication and use  $t_{\text{evol}}$  as the remaining lifetime for the planets. To fix ideas, consider a planet in a 4-day orbit around a solar type star with  $Q_* = 10^6$ . For a planet with the mass of  $m = 1 m_J$  ( $10 M_{\oplus}$ ), the evolutionary time  $t_{\text{evol}} \approx 6$  Gyr (180 Gyr). Low mass planets can thus survive a long time in tight orbits. This finding suggests the stellar spin correction (e.g., see Hut 1981) to equation (60) will generally be small: For super-Earth-mass planets, in order for the evolution time to be less than the age of the universe, the orbital period must be substantially less than 4 days; in contrast, the typical stellar spin periods are much longer (McQuillan et al. 2013).

Figure 8 shows the time scales  $t_{\text{evol}}$  for our observed sample of planets to spiral in to their host stars according to equations (60), (61), and (62). These time scales, which are given in Gyr, are plotted versus the current orbital periods. This figure shows the resulting time scales for the subsample of systems that are unstable and have stellar periods longer than the orbital periods (if this second criterion is not met, the planets would spiral outwards). For completeness, we include the correction for the fact that the stellar rotation rate is not zero (Hut 1981), but it has little effect on the results. For the sake of definiteness, Figure 8 is constructed using the typical value  $Q_* = 10^6$  for the tidal quality parameter of the star. With this value for  $Q_*$ , the majority of planetary systems have lifetimes in excess of 1 Gyr; only 14 of the planets (2.6% of the subsample) are scheduled to be accreted within this time. For comparison, the ages of the stars are typically in the range 1 – 6 Gyr. This finding is sensible: One expects a small fraction of the planets to have short remaining lifetimes.

Although the small number of planets with small

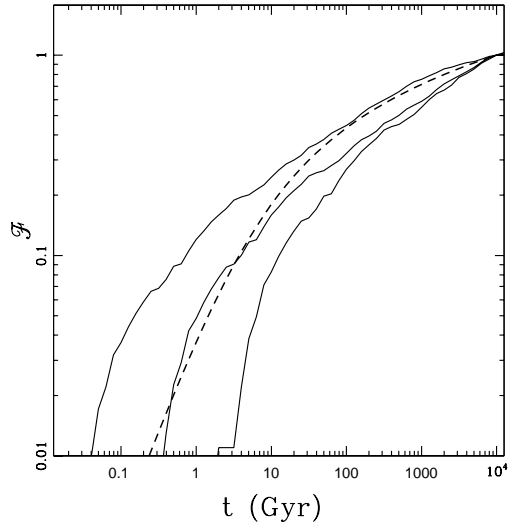


**Figure 9.** Distribution of decay times for the planet sample. For the observed planets in the sample, the solid curves show the cumulative probability distribution for the time required to spiral into the host star (limited to  $t \leq 10^4$  Gyr). The three curves show the projected results for different choices of the stellar tidal dissipation parameter  $Q_* = 10^7$  (top),  $10^6$  (middle), and  $10^5$  (bottom). The dashed curve shows the expected cumulative distribution for an ensemble of systems with an initial distribution that is uniform in  $\log(t)$  with ages in the range 1 – 6 Gyr.

projected survival times seems sensible, we can test this idea further by constructing probability distributions. In order to proceed, however, we must specify the starting distribution, which is unknown. The current observational data-base for extrasolar planets shows that the distribution of orbital periods or semimajor axis is log-random to leading order. As a benchmark example, we thus suppose that the starting distribution of survival times  $t_0$  is log-random, i.e.,

$$\frac{dP}{d\xi} = \mathcal{N} = \text{constant} \quad \text{where} \quad \xi \equiv \log t_0, \quad (63)$$

where  $t_0$  is the time required for a planet to spiral into its host star from its starting orbit and where  $\mathcal{N}$  is the normalization constant. If  $\Delta t$  is the age of the system, then the time required to spiral into the star from the current configuration is given by

$$t = t_0 - \Delta t. \quad (64)$$

Next we define

$$\eta = \log t = \log [t_0 - \Delta t], \quad (65)$$

and find the probability distribution for the current set of survival times

$$\frac{dP}{d\eta} = \mathcal{N} \frac{e^\eta}{e^\eta + \Delta t} = \mathcal{N} \frac{t}{t + \Delta t}. \quad (66)$$

This expression would provide the probability distribution if all of the systems have the same age  $\Delta t$ . We can

include an age spread by assuming that the system ages are uniform distributed between a minimum age  $\tau_1$  and a maximum age  $\tau_2$ . The observed age distribution for *Kepler*-planet-hosting stars extends from roughly  $\tau_1 \approx 1$  Gyr to  $\tau_2 \approx 6$  Gyr, although it is weighted toward the lower end of the range (Walkowicz & Basri 2013; see also Lanza & Shkolnik 2014). The averaged probability distribution then takes the form

$$\left\langle \frac{dP}{d\eta} \right\rangle = \mathcal{N}' \frac{t}{\tau_2 - \tau_1} \log \left[ \frac{t + \tau_2}{t + \tau_1} \right], \quad (67)$$

where  $\mathcal{N}'$  is the new normalization constant. The cumulative probability is then given by

$$P(\eta) = \mathcal{N}' \left[ (t + \tau_2) \log(t + \tau_2) - (t + \tau_1) \log(t + \tau_1) - \tau_2 \log(\tau_2) + \tau_1 \log(\tau_1) \right]. \quad (68)$$

Figure 9 shows the cumulative distribution of survival times for both the data and the theoretical considerations outlined above. Distributions are determined from the observational sample by using different values for the tidal quality factor  $Q_* = 10^5$ ,  $10^6$ , and  $10^7$ . As shown in the figure, the distributions obtained with these values of  $Q_*$  bracket the probability distributed calculated using the expression of equation (68). More specifically, the data do not favor low values of  $Q_* \approx 10^5$  (cf. Teitler & Königl 2014), but rather indicate that the tidal quality factor lies in the range  $Q_* = 10^6 - 10^7$ .

## 6 CONCLUSION

This paper has considered the stability of tidal equilibria for planetary systems with two coupled objectives. First, we have applied existing stability criteria (Hut 1980) to a subcollection (McQuillan et al. 2013) of the candidate planetary systems discovered by the *Kepler* mission (Batalha et al. 2013). Second, we have generalized the classic stability problem to include a quadrupole moment for the central star. These results indicate that planetary systems are generally not in — or near — tidal equilibrium states.

### 6.1 Summary of Results

We have applied existing stability criteria to observed exoplanet candidates (Section 3) by considering the innermost planet and the star as the planetary system. Stability requires that the orbital period is the same as the stellar rotational period (equation [15]; Hut 1980). Observed systems are generally far from synchronous (Figure 3); most cases have longer stellar periods, but some stars are rotating faster than their planetary orbits. Stability also requires that the system has sufficiently large total angular momentum (equation [17]) and that at least three-fourths of the angular momentum is contained in the orbit (equation [24]). We find that most planetary systems in the sample have enough angular momentum for a stable equilibrium to exist (Figure 4), but that most planetary systems are not actually in their equilibrium config-

uration. The majority of the planetary systems have too little orbital angular momentum for stability (Figure 5).

In order for a planetary system to reside in a stable tidal equilibrium state, it must have enough total angular momentum (equation [17]) and enough orbital angular momentum relative to the total (equation [24]). These conditions can be combined to obtain a necessary — but not sufficient — condition for stability (equations [28] and [30]). This new requirement can be evaluated without knowing the spin rate of the star, and hence can be applied to a wider sample of observed systems. Moreover, Figure 6 shows that most systems which satisfy this necessary constraint also meet the more rigorous constraints.

We have generalized the stability calculation to include the effects of a stellar quadrupole moment (Section 4). Stability again requires synchronous rotation, where the orbital period includes the quadrupole correction (equation [39]). As before, stability requires that the total angular momentum is larger than a threshold value (equation [43]) and that a sufficiently large fraction of the total angular momentum is carried by the orbit (equation [53]). However, this quadrupole correction is too small to change the conclusion that most of the observed planetary systems are not in a tidal equilibrium state.

Given that most observed systems (in our sample) are not in tidal equilibrium, we consider their possible time evolution in Section 5. These considerations show that the time required for planets to be accreted onto their host stars is almost always longer than the age of the system (Figure 8). However, some fraction ( $\sim 2.6\%$ ) of the planetary systems have short evolutionary time scales ( $t_{\text{evol}} < 1$  Gyr) and are expected to be short-lived. To assess the consistency of this finding, we have constructed probability distributions for the survival times (Figure 9). If the tidal quality factor of the stars lies in the range  $Q_* = 10^6 - 10^7$ , then the observed/inferred distribution of survival times can be explained with a simple model where the planets start with a log-random distribution of initial survival times (basically, a log-random period distribution) and evolve according to leading order tidal dissipation theory (equations [60] and [61]).

## 6.2 Discussion

The results of this work apply to the particular sample of 738 candidate planetary systems for which we have measured rotational periods for the stars (McQuillan et al. 2013). However, observational biases could be present. The results presented here assume that the stars are rotating as solid bodies with their reported rotation rates, and have a single value of the dimensionless moment of inertia  $\chi = I/(MR^2)$ . The critical angular momentum scales as  $L_X \propto I^{1/4}$ , so these variations are not expected to influence the conclusions. Nonetheless, it remains possible for only the outer layers of the star to participate in rotation, so that the stellar moment of inertia would be much smaller. In this case, the star would have less angular momentum for a given rotation rate, so that the criterion of equation (24) would be more easily satisfied.

The constraints found for the tidal quality factor  $Q_*$  are also subject to uncertainties. The evolutionary sce-

nario presented in Section 5 is not unique because the initial period distribution is not measured and is not necessarily log-random. The planetary orbits could also start with nonzero eccentricities, which would lead to different initial evolutionary paths (although the paths eventually converge). Additional effects could also influence the results, including magnetic coupling with the star, stellar braking through mass-loss, and interactions with additional planets in the system. All of these issues should be addressed in future work and as more data become available. Nonetheless, this paper shows that the simplest scenario — a log-random initial period distribution and  $Q_* \sim 10^6$  — is consistent with the current *Kepler* data.

One basic result of this study is that the observed planetary systems are generally not in tidal equilibrium states. Moreover, most systems are apparently far from equilibrium. Tidal equilibrium implies synchronous states, but Figure 3 shows that stellar rotation periods and orbital periods are generally not equal and are not even strongly correlated. Stability also requires that the orbital angular momentum exceed the spin angular momentum by a factor of 3, but Figure 5 shows that most systems fall short of this benchmark by factors of 10 to 100. In the presence of dissipation — from any source, not only the simple tidal model encapsulated by equation (60) — one expects systems to evolve toward an equilibrium state.

Taken together, the findings summarized above argue for two properties of these planetary systems. The first property is that any coupling between the stars and the planets is weak. Typically, these systems are dynamically old, having experienced of order  $10^{11}$  orbits, and yet they still are not even close to an equilibrium state. The second property is that the formation mechanism is largely independent of tidal equilibrium considerations. The planetary systems are produced so far from their tidal equilibrium states that they almost always remain far away after  $\sim 10^{11}$  orbits.

**Acknowledgments:** We would like to thank Konstantin Batygin and Norm Murray for useful discussions. We also thank an anonymous referee for constructive criticism that improved the paper. AMB is supported by grants NSF-DMS-1207693 and INSPiRE-1343720. Part of this work was carried out during the 2014 International Summer Institute for Modeling in Astrophysics (ISIMA), which focused on gravitational dynamics, and was hosted by the Canadian Institute for Theoretical Astrophysics (CITA). We are grateful for the hospitality and resources of CITA, ISIMA, and Univ. Michigan.

## REFERENCES

- Adams, F. C., & Laughlin, G. 2006, *ApJ*, 649, 1004
- Agol, E., Steffen, J., Sari, R., & Clarkson, W. 2005, *MNRAS*, 359, 567
- Barnes, J. W., & O’Brien, D. P. 2002, *ApJ*, 575, 1087
- Batalha, N. M., Rowe, J. F., Bryson, S. T., et al. 2013, *ApJS*, 204, 24
- Batygin, K., & Adams, F. C. 2013, *ApJ*, 778, 169
- Bellerose, J. & Scheeres, D. J. 2008, *Celest. Mech. Dynam. Astr.*, 100, 63

- Bloch, A. M., Krishnaprasad, P. S., Marsden, J. E., & Ratiu, T. S. 1994, *Ann. Inst. H. Poincaré, Analyse Non-lineaire*, 11, 37
- Counselman, C. C. 1973, *ApJ*, 180, 307
- Čuk, M., Ragozzine, D., & Nesvorný, D. 2013, *AJ*, 146, 89
- Danby, J.M.A. 1968, *AJ*, 73, 1031
- Darwin, G. H. 1879, *The Observatory*, 3, 79
- Darwin, G. H. 1880, *Phil. Trans. R. Soc. A*, 171, 713
- Goldreich, P. M., & Soter, S. 1966, *Icarus*, 5, 375
- Goldstein, H. 1950, *Classical Mechanics* (Cambridge: Addison-Wesley)
- Hartle, J. B. 2003, *Gravity: An Introduction to Einstein's General Relativity* (San Francisco: Addison Wesley)
- Heller, R., Leconte, J., & Barnes, R. 2011, *A&A*, 528, 27
- Hesse, L. O. 1872, *Die Determinanten elementar behandelt* (Leipzig)
- Holman, M. J., & Murray, N. W. 2005, *Science*, 307, 1288
- Hut, P. 1980, *A&A*, 92, 167
- Hut, P. 1981, *A&A*, 99, 126
- Lanza, A. F., & Skholnik, E. L. 2014, *MNRAS*, 443, 1451
- Levrard, B., Winisdoerffer, C., & Chabrier, G. 2009, *ApJ*, 692, 9
- Lissauer, J. J., Ragozzine, D., Fabrycky, D. C. et al. 2001, *ApJS*, 197, 8
- McQuillan, A., Mazeh T., Aigrain S. 2013, *ApJ*, 775, 11
- Miralda-Escudé, J. 2002, *ApJ*, 564, 1019
- Morbidelli, A. 2002, *Modern Celestial Mechanics: Aspects of Solar System Dynamics* (London: Taylor & Francis)
- Murray, C. D., & Dermott, S. F. 1999, *Solar System Dynamics* (Cambridge: Cambridge Univ. Press)
- Penev, K., Jackson, B., Spada, F., & Thom, N. 2012, *ApJ*, 751, 96
- Postnov, K. A., & Yungelson, L. R. 2006, *LRR*, 9, 6
- Ragozzine, D., & Brown, M. E. 2009, *AJ*, 137, 4766
- Scheeres, D. J. 2002, *Icarus*, 159, 271
- Scheeres, D. J. 2009, *Celest. Mech. Dynam. Astr.*, 104, 103
- Schlaufman, K. C., & Winn, J. N. 2013, *ApJ*, 772, 143
- Simo, J. C., Lewis, D. K., & Marsden, J. E. 1991, *Arch. Rat. Mech. Anal.*, 115, 15
- Taam, R. E., King, A. R., & Ritter, H. 2000, *ApJ*, 541, 329
- Taam, R. E., & Sandquist, E. L. 2000, *ARA&A*, 38, 113
- Teitler, S., & Königl, A. 2014, *ApJ*, 786, 139
- Walkowicz, L. M., & Basri, G. S. 2013, *MNRAS*, 436, 1883
- Wang, L.-I., Krishnaprasad, P.S., & Maddocks, J.H. 1991, *Celest. Mech. Dyn. Astron.* 50, 349
- Weiss, L. M., Marcy, G. W., Rowe, J. F., et al. 2013, *ApJ*, 768, 14
- Zahn, J. P. 1977, *A&A*, 41, 329
- Zhang, M., & Penev, K. 2014, *ApJ*, 787, 131